Structural and Electronic Properties of $Li_2B_4O_7$

Mazharul M. Islam,[†] Volodymyr V. Maslyuk,[‡] Thomas Bredow,*[,†] and Christian Minot[§]

Theoretische Chemie, Universität Hannover, Am Kleinen Felde 30, 30167 Hannover, Germany, Institut für Festkörperphysik, Universität Hannover, Appelstr. 2, 30167 Hannover, Germany, and Laboratoire de Chimie Théorique, UMR 7616 CNRS, Université P. et M. Curie Case 137, Tour 23-22, 4 Place Jussieu, Paris 75252 Cédex 05, France

Received: November 19, 2004; In Final Form: May 18, 2005

The reliability of various quantum-chemical approaches for the calculation of bulk properties of lithium tetraborate $Li_2B_4O_7$ was examined. Lattice parameters and the electronic structure obtained with density-functional theory (DFT), with DFT−Hartree−Fock (HF) hybrid methods, and with the semiempirical method MSINDO were compared to available experimental data. We also compared the results at DFT level using different wave functions, either based on linear combinations of atom-centered orbitals (LCAO), or on plane waves, as implemented in the crystalline orbital programs CRYSTAL and VASP. The basis set dependence of calculated properties was investigated for the LCAO method. In the plane wave approach ultrasoft pseudopotentials (US PP), and projector-augmented wave (PAW) potentials were used to represent the core electrons. For all methods under consideration, the calculated $Li_2B_4O_7$ structure parameters are close to each other and agree within a few percent with measured values. A more pronounced method dependence was found for the band structure, the band gap and the cohesive energy. Closest agreement between theoretical and experimental results for the band gap was obtained with the DFT−HF hybrid methods while pure DFT methods underestimate and HF based methods overestimate the measured value. It was found that the calculated band gap strongly depends on the atomic basis set in the LCAO approach. The description of the core electrons considerably affects the cohesive energy obtained with the plane wave approach. Atomic charges based on a Mulliken analysis were compared to effective charges obtained from Raman spectroscopy. Electron density maps are used to analyze the character of B−O and Li−O interactions.

1. Introduction

In recent years, many investigations have been conducted on crystalline lithium tetraborate (LTB) $Li_2B_4O_7$ due to its important physical properties, such as a high coefficient of electrochemical coupling, a low velocity of propagation of surface acoustic waves, zero thermal expansion coefficient, high mechanical strength, and low electrical conductivity at room temperatures. It is used for laser radiation converters,[1] as piezoelectric nonlinear optical device for second harmonic generation,[2−4] in electroacoustic devices,[5−7] and as a pyroelectric sensor.[7] LTB was also found to be a Li^+ ion conductor along the (001) direction (polar axis) at high temperatures.[8−14] In addition, Mn- or Cu-doped $Li_2B_4O_7$ crystals are used as tissue-equivalent thermoluminescence dosimeters.[15]

The LTB lattice belongs to space group $I4_1cd$ and has 104 atoms per crystallographic unit cell.[16] The measured lattice parameters are $a = 9.48$ Å and $c = 10.29$ Å. The main structural pattern is a $[B_4O_9]^{6-}$ complex which consists of two planar trigonal (BO_3) and two tetrahedral (BO_4) units. The lithium atoms are located at interstices.[16] A limited number of experimental investigations on the electronic structure[17−19] are available in the literature.

In this paper, a theoretical investigation of $Li_2B_4O_7$ bulk properties, such as lattice constants, bond distances, cohesive energy, the electronic structure, and the charge density distribution, is performed. The present work is motivated by recent experimental studies of nanocrystalline $Li_2O-B_2O_3$ composites[20,21] where a high Li mobility along the phase boundaries was found. LTB is considered as a model system for the interface region between Li_2O and B_2O_3 nanoparticles. This study provides the basis for further theoretical studies of Li migration in LTB and $Li_2O-B_2O_3$ composites. The reliability of several quantum-chemical methods at different levels of theory for the reproduction of available experimental data on LTB bulk properties is examined since an accurate description of the bulk is a necessary prerequisite for the study of defects. We also investigate the influence of technical aspects of the quantum-chemical calculations, in particular the basis sets used for the construction of the crystalline orbitals, and the description of core electrons, and the cutoff energy in plane wave approaches.

2. Computational Methods

Bulk properties of LTB were obtained with periodic calculations at DFT level, and with the semiempirical method MSINDO. The Perdew−Wang correlation functional based on the generalized gradient approximation (PWGGA),[22] is combined with three different exchange functionals. In the HF+PW hybrid approach the exact HF exchange formulation is used. The exchange functional of the hybrid method PW1PW is a linear combination of the HF expression (20%) and the PW exchange functional (80%).[23] The third approach is the original PWGGA DFT method.[22,24] The latter two methods have been

* Corresponding author. E-mail: bredow@mbox.theochem.uni-hannover.de.
[†] Theoretische Chemie, Universität Hannover.
[‡] Institut für Festkörperphysik, Universität Hannover.
[§] Université P. et M. Curie Case 137.

10.1021/jp044715q CCC: $30.25
Published on Web 06/25/2005

applied for calculations of bulk properties of MgO, NiO, CoO,[23] and TiO_2.[25] In these studies, good agreement between calculated and experimental bulk properties was observed, in particular for the PW1PW hybrid method. For comparison, we also used the well-known B3LYP hybrid method.[26] These DFT approaches were used as implemented in the crystalline orbital program CRYSTAL03.[27] In CRYSTAL the Bloch functions are linear combinations of atomic orbitals (LCAO). The quality of the atomic basis sets determines the reliability of the results. Therefore, we used two different basis sets for the elements. In basis set A, a 6−11G[28] basis was used for Li. This is an extension of the 6−1G basis[29] where the outer exponent has been optimized in $Li(OH)H_2O$. For boron, we used a 6-21G* basis[30] which is a modification of the original 6-21G[31] basis set, where the outer sp exponent was optimized for solid BN. For oxygen, a 8-411G*[32] basis set was used as developed for crystalline metal oxides. In the extended basis set B, the following basis sets were used for the elements: 7-11G* on Li,[33] 6-21G(2d) on B with an additional polarization function, and again 8-411G* on O. We did not find a significant effect by further increasing the O basis set, but at the same time we encountered severe SCF convergence problems.

The Perdew−Wang (PWGGA) exchange-correlation functional[22,24] was also used with the plane wave program VASP.[34−36] In this way, the effect of different kinds of basis sets, atom-centered and delocalized plane waves, on the results obtained with the same density-functional method, could be studied. In contrast to the LCAO approach, which allows the explicit treatment of all electrons, inner electrons are replaced by effective potentials in plane wave methods. To study the effect of the treatment of core electrons on calculated LTB properties, we used two different potentials, ultrasoft (US) pseudopotentials[37,38] and projector augmented wave (PAW) potentials.[39,40] The valence electrons were treated with plane wave sets with energy cutoffs of 520 eV (PWGGA-PAW approach), and 515 eV (PWGGA-US approach). These values are obtained by multiplying the standard values[41] by 1.3. In selected cases, the dependence of calculated bulk properties from the cutoff energy was studied.

We also investigated the reliability of the semiempirical method MSINDO[42,43] for the description of LTB bulk properties by comparison to the first-principles methods and to experiment. Because of their computational efficiency, semiempirical methods allow the treatment of much larger and therefore more realistic model systems compared to first-principles methods. It is planned to exploit this in future studies of defect formation and migration in LTB and $Li_2O-B_2O_3$ nanocompounds.

MSINDO is a modification of the previous version SINDO1.[44] Both methods are based on the INDO approximation. Only two-center interaction integrals are taken into account. One-electron integrals are transformed according to a Löwdin orthogonalization of the basis. A minimal set of Slater-type functions is used to describe the valence orbitals. Inner orbitals are taken into account by Zerner's pseudopotential.[45] More details about the methods can be found elsewhere.[42−46] Both methods MSINDO and SINDO1 have been applied to a number of studies of bulk, surface, and adsorption properties on a variety of metal oxides.[47−57] It was shown that they provide results for bulk, surface and adsorption properties in good agreement with experiment and with high-level ab initio and DFT methods.

The LTB bulk was modeled with MSINDO using the recently implemented cyclic cluster model (CCM).[58,59] In this model periodic boundary conditions are directly applied to a cluster of moderate size. A CCM calculation is similar to a supercell calculation at Γ point, but with an interaction region that is defined by the cluster dimension and not by cutoff thresholds. In this way a balanced summation of Coulomb and exchange integrals is achieved which in general leads to fast convergence with increasing cluster size. A comparison of the supercell approach and the CCM was given recently.[60]

3. Results and Discussion

In this section, we present the results for LTB bulk structure relaxation, cohesive energy, electronic properties such as band gap, electron density of states (DOS), and charge distribution, and compare with available literature data. Atomic Mulliken charges are compared with charges derived from the longitudinal optical (LO) and transverse optical (TO) splitting in Raman spectra.[61]

3.1. Structure Optimization. The optimized lattice parameters and bond distances and angles as obtained with HF+PW, PW1PW, PWGGA, and B3LYP using CRYSTAL, with PWGGA-US, PWGGA-PAW using VASP, and with MSINDO, are given in Table 1 together with the corresponding experimental values.[16] The numbering of the Li, B, and O atoms is shown in Figure 1. In the MSINDO structure optimization, the cyclic cluster $Li_{16}B_{32}O_{56}$ was used, which corresponds to the conventional unit cell of LTB (Figure 1). First a full optimization of atomic fractional coordinates was performed keeping the lattice vectors fixed at the experimental values. Starting from the then obtained internal coordinates, the lengths of the lattice vectors were optimized. This procedure was repeated iteratively until the forces were smaller than 0.02 eV/Å. A similar optimization of all coordinates of the primitive LTB unit cell $Li_8B_{16}O_{28}$ was performed with CRYSTAL03 using basis set A and with VASP using both PAW and US PP potentials.

For all considered methods, the deviation between calculated and measured lattice parameters is less than 1.8% (Table 1). Among the DFT-type methods, the HF+PW method gives the worst lattice parameters. The length of a is underestimated by 0.08 Å and that of c is underestimated by 0.19 Å. This is in line with previous investigations of MgO and other cubic oxides using a combination of HF exchange and DFT correlation.[23] Best agreement for a and c is obtained with the two hybrid methods PW1PW ($\Delta a = +0.02$ Å, $\Delta c = +0.03$ Å) and B3LYP ($\Delta a = +0.04$ Å, $\Delta c = +0.01$ Å).

The results of the LCAO implementation (in CRYSTAL) and the plane wave implementations (PWGGA-US, PWGGA-PAW in VASP) of the PWGGA method are relatively similar. This is particularly the case if ultrasoft pseudopotentials are used (PWGGA-US). Here the differences between CRYSTAL and VASP results are smaller than 0.01 Å. The deviations from experiment are between 0.04 and 0.05 Å. Surprisingly, the PWGGA-PAW approach gives the worst lattice parameters, namely a is overestimated by 0.09 Å and c is overestimated by 0.10 Å. This is not in line with the general observation that the PAW potential leads to improved geometries compared to US pseudopotentials.[39] We, therefore, investigated the dependence of E_{cut} for lattice parameters, cohesive energy and band gap (Table 2) for PWGGA-PAW and PWGGA-US methods. In both approaches a considerable increase of a and c occurred when the default values of E_{cut} (396 and 400 eV, respectively) were multiplied by 1.3 (515 and 520 eV, respectively). The changes are about +0.15 Å for PWGGA-PAW and +0.11 Å for PWGGA-US. The cohesive energy per LTB (E_{coh}) changes by +10 kJ/mol for PWGGA-PAW and by +60 kJ/mol for PWGGA-US whereas the change of the band gap is negligible. The further investigation with an increased value of E_{cut} by

TABLE 1: Structural Properties of Solid $Li_2B_4O_7$ Giving a Comparison of Calculated and Experimental Lattice Vectors *a* and *c*, Bond Distances (Å), and Angles (deg) (for the Numbering of the Atoms, See Figure 1)

parameter	HF + PW[a]	PWGGA[a]	PWGGA-PAW[b]	PWGGA-US[b]	PW1PW[a]	B3LYP[a]	MSINDO	expt[c]
				Lattice Parameters				
a	9.40	9.53	9.57	9.52	9.50	9.52	9.44	9.48
c	10.10	10.32	10.39	10.33	10.32	10.30	10.44	10.29
				Bonds (Å)				
B_1-O_1	1.321	1.372	1.365	1.363	1.361	1.362	1.360	1.355
B_1-O_2	1.339	1.393	1.381	1.377	1.378	1.384	1.385	1.371
B_1-O_3	1.349	1.396	1.386	1.383	1.381	1.388	1.371	1.374
B_2-O_1	1.419	1.470	1.454	1.441	1.463	1.464	1.442	1.452
B_2-O_2	1.465	1.527	1.522	1.528	1.510	1.517	1.488	1.506
B_2-O_3	1.459	1.517	1.517	1.515	1.508	1.512	1.498	1.501
B_2-O_4	1.433	1.463	1.464	1.458	1.451	1.451	1.447	1.454
$Li-O_1$	2.171	2.153	2.107	2.303	2.082	2.079	2.394	2.170
$Li-O_2$	1.940	1.974	1.979	1.826	1.966	1.970	2.027	1.967
$Li-O_3$	1.974/2.077	2.012/2.082	2.018/2.102	1.836/2.051	2.005/2.086	1.995/2.085	2.102/2.103	2.027/2.080
				Angles (deg)				
$B_1-O_1-B_2$	129	124	126	125	125	125	126	126
$B_1-O_2-B_2$	117	115	115	115	116	115	119	116
$B_1-O_3-B_2$	120	119	119	119	119	119	121	120
$B_2-O_4-B_2$	108	108	109	109	109	109	110	109

[a] Obtained with CRYSTAL03. [b] Obtained with VASP. [c] Reference 16. HF + PW: exchange 100% HF; correlation 100% Perdew-Wang. PWGGA: exchange 100% Perdew-Wang; correlation 100% Perdew-Wang. PW1PW: exchange 20% HF and 80% Perdew-Wang; correlation 100% Perdew-Wang. B3LYP: exchange 20% HF and 80% Becke; correlation 100% Lee−Yang−Parr.

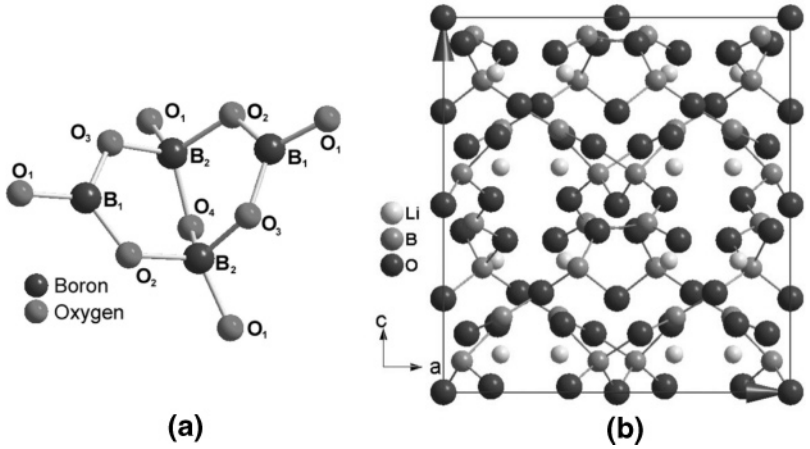

Figure 1. Main structure element of bulk LTB (anion $[B_4O_9]^{4-}$) consisting of $B_{(1)}O_3$ and $B_{(2)}O_4$ units (a) and the unit cell of $Li_2B_4O_7$ (b).

TABLE 2: Dependence of Calculated LTB Lattice Parameters *a*, *c* (Å), Cohesive Energy E_{coh} (kJ/mol) per LTB and Band Gap E_g (eV) Obtained with PWGGA-PAW and PWGGA-US (VASP) from the Energy Cutoff E_{cut} (eV) Used for the Plane Wave Expansion of the Wave Function

PWGGA-PAW approach					PWGGA-US approach				
E_{cut}	*a*	*c*	E_{coh}	E_g	E_{cut}	*a*	*c*	E_{coh}	E_g
400	9.42	10.22	−8137	6.18	396	9.41	10.22	−7998	6.19
520	9.57	10.39	−8127	6.22	515	9.52	10.33	−7932	6.26
600	9.56	10.38	−8119	6.17	594	9.51	10.32	−7932	6.20

multiplying the default values with 1.5 (600 eV for PWGGA-PAW and 595 eV for PWGGA-US) showed that the geometry, cohesive energy (E_{coh}) and band gap (E_g) are already converged with $E_{cut} = 520$ and 515 eV, respectively (Table 2). Since plane wave calculations with larger cutoff energy are computationally more costly, we used $E_{cut} = 520$ eV for PWGGA-PAW and $E_{cut} = 515$ eV for PWGGA-US throughout in the following, if not stated otherwise.

With MSINDO, the lattice parameter *a* is underestimated by 0.04 Å and *c* is overestimated by 0.15 Å. These deviations are in the range of the errors of the first-principles methods.

The calculated bond lengths and angles for all methods agree well with the experimental values (Table 1). The deviation of calculated and measured boron−oxygen bond distances for 3-fold coordinated boron atoms (B_1, see Figure 1) does not exceed 0.035 Å. The best agreement was found for PWGGA-PAW and PWGGA-US, where the deviation is not more than 0.01 Å. Here, the LCAO-based PWGGA implementation gives slightly different results; all B_1-O bond lengths are larger than the corresponding experimental values, and the largest error is 0.02 Å. This can be due to incompleteness of the atomic basis sets of basis A. For PW1PW and B3LYP, the deviation of B_1-O bond lengths is less than 0.015 Å, while HF+PW gives too small values (by up to −0.035 Å). The semiempirical method MSINDO performs in a manner similar to the hybrid methods.

The same trends were observed for the B_2-O bond lengths, where the boron atom is 4-fold coordinated. The experimentally obtained distances B_2-O_2 and B_2-O_3 are larger than the corresponding distances B_2-O_1 and B_2-O_4.

The four lithium−oxygen distances range from 1.94 to 2.18 Å.[16] The worst result for these bond lengths is obtained by the semiempirical method, where the error for the $Li-O_1$ bond (Table 1) is 0.22 Å. Among the DFT methods, PWGGA-US gives the worst values of lithium−oxygen distances. The $Li-O_1$ bond length is overestimated by 0.13 Å and $R(Li-O_3)$ is underestimated by 0.19 Å. A possible explanation is that the

TABLE 3: Comparison of Calculated Cohesive Energies E_{coh} Per $Li_2B_4O_7$ Unit (kJ/mol) Obtained with Different Methods with Experimental Heat of Atomization

method	HF + PW[a]	PWGGA[a]	PWGGA-PAW[b]	PWGGA-US[c]	PW1PW[a]	B3LYP[a]	MSINDO	expt[d]
E_{coh}	−7241	−7840	−8119	−7932	−7674	−7450	−8128	−7658

[a] CRYSTAL results with basis set A. [b] VASP results with cutoff energy 600 eV. [c] VASP results with cutoff energy 594 eV. [d] Reference 62.

US pseudopotential gives an insufficient description of the Li core electrons and this deficiency is partly removed by the PAW potential where deviations of R(Li−O) are much smaller (Table 1).

For all calculated bond angles in the LTB crystal, we found good agreement of calculated values with experimental data. The errors are smaller than 2.6%. For briefness we have restricted the comparison of calculated and experimental angles to $B_1-O_1-B_2$, $B_1-O_2-B_2$, $B_1-O_3-B_2$, and $B_2-O_4-B_2$ (Table 1) The agreement for the other angles is similar.

3.2. Binding Energy. In the following, we compare the cohesive energies E_{coh} obtained with the theoretical methods with the experimental heat of atomization $\Delta_a H$, −7658 kJ/mol,[62] Table 3. Contributions from the zero point energy are neglected in the calculations. The cohesive energy E_{coh} per $Li_2B_4O_7$ formula unit is calculated by a normalization of the obtained binding energies which are differences of the total energies of the periodic system and the free atoms in their ground states. For the calculation of atomic reference energies with CRYSTAL, the basis sets of the free atoms were optimized by augmenting the basis sets used in the periodic calculations by diffuse sp and d shells until convergence was achieved. For both the PWGGA-PAW and PWGGA-US approaches with VASP, atomic reference energies were calculated with PAW and US pseudo potentials by using pseudo lattice constants of 13 Å for the ^{2}Li atom, 15 Å for the ^{2}B atom, and 8 Å for the ^{3}O atom with energy cutoffs E_{cut} 600 and 594 eV, respectively. The VOSKOWN keyword[63] was used to improve convergence of the atomic ground state energy, as it is important particularly for a GGA-based calculation.[41] In all cases, the atomic reference energies were calculated at unrestricted Kohn−Sham level.

Best agreement with the experimental $\Delta_a H$ is obtained with the PW1PW hybrid method. The calculated cohesive energy is only 25 kJ/mol lower than the measured value. With CRYSTAL PWGGA, the deviation from experiment is considerably larger, −182 kJ/mol. With the same density functional, PWGGA, using plane waves and US pseudopotentials (PWGGA-US), the cohesive energy is more negative by −92 kJ/mol. With PWGGA-PAW (VASP) the difference is even larger, −279 kJ/mol. There are several possible reasons for the differences between LCAO and plane wave based cohesive energies. The total energy of the periodic system can be too high with the LCAO method due to basis set incompleteness, or the atomic reference energies obtained with plane waves are too high. The difference between E_{coh} obtained with PWGGA-PAW and PWGGA-US indicates the influence of the effective potentials in the plane wave program VASP. By performing a single point CRYSTAL PWGGA calculation with the larger basis set B, we checked to see if the smaller cohesive energy was due to LCAO basis set incompleteness. E_{coh} (PWGGA, basis B) is −7824 kJ/mol, very close to the result obtained with basis A. We also carefully tested the convergence of atomic reference energies with respect to the lattice parameter and energy cutoff in the atomic plane wave calculations. The atomic energies of O, Li, and B at UKS level change only by up to 5 kJ/mol with PWGGA-PAW and by less than 10 kJ/mol with PWGGA-US when the standard cutoff energies are increased. This effect cannot account for the observed differences between E_{coh} obtained with the three PWGGA implementations. We therefore conclude that the differences between CRYSTAL and VASP PAW results are mainly due to the description of core electrons. This mainly affects binding energies, while geometry parameters are less sensitive.

The other hybrid method B3LYP gives a cohesive energy that is too small in absolute value by 208 kJ/mol. The error is even larger with HF+PW, 417 kJ/mol (Table 3). This trend is in line with previous studies of MgO, NiO, and CoO.[23] As for the geometry parameters, the MSINDO result for E_{coh} is in the range of the first-principles methods.

3.3. Band Structure and Density of States. Only a small number of theoretical and experimental investigations of electronic spectra for crystalline $Li_2B_4O_7$ were found in the literature.[17−19] The electronic structure, namely the valence band, of LTB, has been experimentally studied by X-ray photoelectron spectroscopy (XPS)[18] in combination with a theoretical investigation based on local density approximation (LDA) calculations of the free anion $[B_4O_9]$.$^{6-}$ The LTB band structure was calculated[19] by a modified LCAO method using symmetrized Bloch functions, but only the results for the valence band were presented. To our best knowledge, there are no experimental and theoretical results in the literature about the value of the band gap (E_g). It is only known that the fundamental absorption edge is 7.3 eV,[17] which is comparable to the value of ≈7.9 eV found by reflection spectroscopy.[19]

The band structure was calculated along the path that contains the highest number of high-symmetry points of the Brillouin zone[64] ($M \rightarrow \Gamma \rightarrow X \rightarrow P \rightarrow N$). The results of calculation of electronic structure for the PW1PW method using basis set B are shown in Figure 2. This method was chosen since it gave best agreement with experiment for the electronic structure of MgO, NiO, and CoO.[23] The other methods give the same qualitative band structure, only the bands are shifted therefore the value of the band gap changes, as will be shown below. In Figure 2a, the calculated band structure of crystalline $Li_2B_4O_7$ is shown. According to our results, LTB is a wide gap insulator. One can see that both the valence band (VB) and the conduction band (CB) have a small dispersion indicating large effective masses for the charge carriers as found for similar crystals α-B_2O_3, β-B_2O_3,[65] and LiB_3O_5.[66]

With all considered DFT methods, the top of the VB is at point M, and the bottom of the CB is at Γ. Calculated values of the different methods for vertical VB−CB transitions in $Li_2B_4O_7$ and minimal transition energies are presented in Table 4. The results of CRYSTAL DFT methods are obtained with both basis sets A and B. Since a structure optimization with basis B is computationally demanding, we used the optimized geometries obtained with basis A.

All considered methods indicate that the LTB crystal has an indirect ($M-\Gamma$) band gap E_g. However, the direct Γ−Γ transition energy is only slightly larger. The difference does not exceed 0.05 eV. The values of E_g vary from 6.22 eV (PWGGA-PAW) to 17.68 eV (HF+PW). The use of HF exchange potential results in a large overestimation of the gap compared to all other methods. The results obtained with the hybrid methods PW1PW and B3LYP are comparable, the difference is only about 0.05 eV.

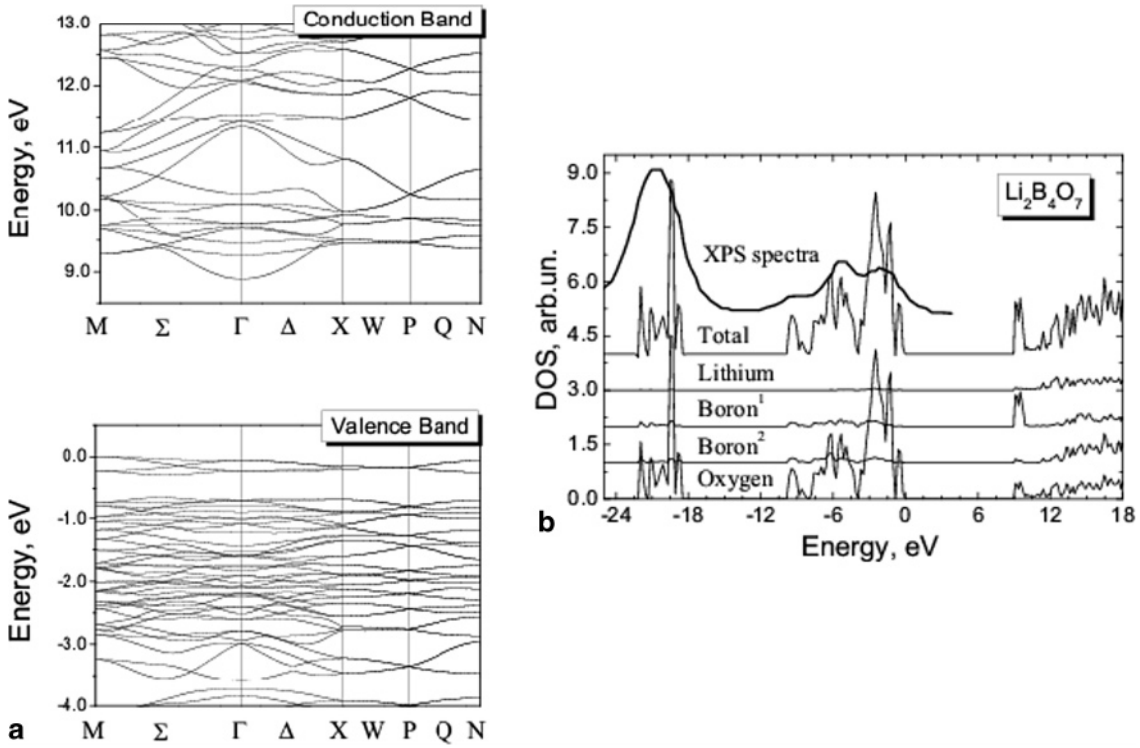

Figure 2. Band structure (a) and density of states (b) of solid $Li_2B_4O_7$ obtained with the PW1PW method using basis set B. For comparison the X-ray photoelectron spectrum[18] is also shown in part b. The experimental XP spectrum was shifted to the top of the valence band which corresponds to $E = 0$.

TABLE 4: Values of Vertical Electronic Transitions and Minimal Transition (MT) Energies E_T^{min} (eV) for $Li_2B_4O_7$ Calculated with Different Methods (Comparison of Basis Sets A and B)

		HF + PW		PWGGA				PW1PW		B3LYP		
transition		A	B	A	B	PWGGA-PAW	PWGGA-US	A	B	A	B	MSINDO
G	G	18.31	17.75	7.15	6.80	6.27	6.31	9.41	8.94	9.37	8.91	
N	N	19.02	18.47	7.24	7.15	7.08	7.10	9.55	9.43	9.54	9.42	
P	P	19.32	18.81	7.40	7.31	7.31	7.34	9.75	9.64	9.71	9.60	
X	X	19.31	18.66	7.35	7.27	7.22	7.24	9.72	9.61	9.67	9.56	
M	M	18.98	18.42	7.19	7.00	6.96	6.99	9.42	9.29	9.40	9.27	
MT		M−Γ	M−Γ	M−Γ	M-Γ	M−Γ	M−Γ	M−Γ	M−Γ	M−Γ	M−Γ	
	E_T^{min}	18.28	17.68	7.11	6.76	6.22	6.26	9.31	8.88	9.32	8.85	9.70

The three PWGGA implementations, CRYSTAL PWGGA, PWGGA-PAW, and PWGGA-US (VASP), give similar values of the transition energies except for the Γ−Γ transition (Table 4). For PWGGA-US and PWGGA-PAW, the Γ−Γ transition energies are very close, 6.31 and 6.27 eV, respectively. This is considerably smaller than the 6.8 eV obtained with CRYSTAL PWGGA using the basis set B. The difference is ≈ 0.5 eV, which is responsible for the difference in the value of band gap (6.26 eV for PWGGA-US, 6.22 eV for PWGGA-PAW, and 6.76 eV for PWGGA). By performing the band structure with basis set including an additional polarization function to the Li basis in the basis set B, it was checked whether the difference in Γ−Γ transition energy was due to the LCAO basis set incompleteness. The Γ−Γ transition energy value is 6.79 eV which is nearly equal to that (6.8 eV) with PWGGA using the basis set B.

The atomic basis set has a pronounced effect on the electronic structure. The PWGGA Γ−Γ transition energy is 7.15 eV with basis A which is 0.35 eV larger than that with basis B. A similar difference is found for the band gap. This difference is mainly due to the inclusion of diffuse and polarization functions in the Li and B basis sets. These orbitals are dominating at the lower part of the CB. A closer analysis reveals that the main effect of basis set increase is a lowering of the CB bottom while the VB top is essentially unchanged. The basis set effect is almost independent from the method, as can be seen by the differences obtained with basis A and B for HF+PW, PW1PW, and B3LYP.

To the best of our knowledge, no experimental information about the value of the band gap is available for LTB. Therefore, we make an estimation of E_g (LTB) based on the measured fundamental adsorption (FA) energy, 7.3 eV,[17] and experimental and calculated band gaps and FA energies which are available for other alkali borate crystals.

The band gap of LiB_3O_5 has been calculated at DFT level. The literature values are 6.95,[67] 7.26,[68] and 7.37 eV.[69] For this compound the experimental FA energy is 7.8 eV.[70] In a previous theoretical study of LiB_3O_5[17] an extrapolation scheme was suggested to obtain an estimation for the experimental band gap E_g from the calculated values. In this way $E_g(LiB_3O_5) \approx 9.5$ eV was obtained. Taking into account the similarities between $Li_2B_4O_7$ and LiB_3O_5 for luminescence properties and optical spectra, and that the FA energy (FAE) of LTB is smaller than FAE(LiB_3O_5) by 0.5 eV, we assume that E_g(LTB) is about 9.0 eV. This crude estimation agrees well with the PW1PW and B3LYP results, ≈8.9 eV (Table 4, basis B), whereas the corresponding PWGGA, PWGGA-US and PWGGA-PAW results, 6.76 eV, 6.26 and 6.22 eV, are considerably too small. A large overestimation of E_g is obtained with HF+PW, 17.68

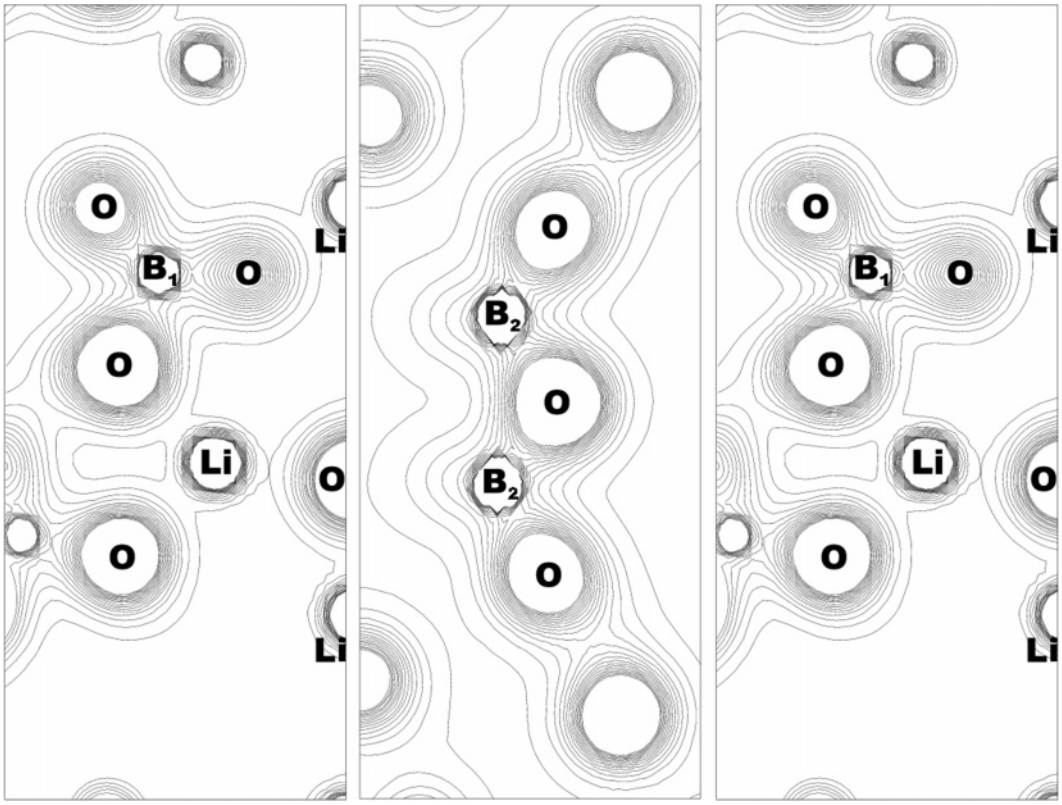

Figure 3. Electronic charge density distribution of $Li_2B_4O_7$ along planes containing $O-B^1-O$ (a), $O-B^2-O$ (b), and O−Li−O (c) angles. The contour lines range from 0.0 to 0.3 e/Å^3 in intervals of 0.02 e/Å^3. B3LYP results are shown.

eV. A similar trend for the agreement of calculated band gaps obtained with HF methods, HF-DFT hybrid methods and pure DFT methods has been found for MgO, NiO, and CoO.[23] The MSINDO band gap, 9.7 eV, is in better agreement with experiment than the corresponding HF+PW, PWGGA, PWGGA-US, and PWGGA-PAW results. Here it has to be noted that the cyclic cluster used for the MSINDO calculations corresponds to a supercell. The Γ point of its reduced Brillouin zone contains Γ and *M* of the primitive Brillouin zone.

The total (TDOS) and projected density of states (PDOS) were calculated at PW1PW level using the Fourier-Legendre technique[71] with a *Monkhorst net*[72] using shrinking factors $s = 8$.

The calculated TDOS of LTB compared with X-ray photoelectron spectrum[18] is shown on Figure 2b. The experimental XPS spectrum was shifted to the calculated Fermi level which corresponds to the VB top in the present case. A good agreement with experiment was obtained for the bandwidths and the interband distances within the VB. The valence bandwidth is about 10 eV. The difference between the upper and lower valence band, which is mainly formed by O 2s states, is about 8 eV.

Analysis of the DOS shows that LTB has very sharp VB and CB edges. The states near the VB top are mainly created by oxygen 2p states. The contributions from atomic orbitals of other atoms (Li, B_1 = boron in BO_3, and B_2 = boron in BO_4) are 10 times smaller than the oxygen PDOS. The bottom of the CB is dominated by contributions from B_1 atoms. It should be noted that orbitals from Li and B_2 atoms are not involved in low-energy band-band transitions since their contributions to the lower part of CB are very small.

3.4. Electronic Charge Density. The electron charge density distribution for the three main types of bonds (B_1-O, B_2-O, Li−O bonds) was calculated. Here we chose the hybrid method B3LYP (basis A) as an example. Test calculations showed that the other methods give a qualitatively similar behavior. We choose three planes containing $O-B^1$-O, $O-B^2$-O and O−Li−O angles. The charge density distribution maps are shown in Figure 3. The contour lines range from 0.0 to 0.3 e/Å^3 with steps of 0.02 e/Å^3.

It can be seen that the charge distribution of oxygen is deformed toward the boron atoms B_1 (Figure 1) and B_2 (Figure 1). This shows that the triangular BO_3 and tetrahedral BO_4 groups have covalent character and as a result the B−O bonds are strong. For the Li−O bonds we observe a different behavior (Figure 1). The charge distribution of both Li and O atoms is almost spherical. The charge density magnitude between these two atoms is small which indicates that the bond is mainly ionic. This is in qualitative agreement with similar analysis of LiB_3O_5.[17] For a more quantitative investigation we performed a Bader-type analysis[73] of the electron density. The critical points (in our case saddle points) of the electron density between B_1-O and B_2-O have different values of charge density ρ_{crit}. The difference $\rho_{crit}(B_1-O) - \rho_{crit}(B_2-O)$ is 0.04 e/Å^3. This indicates that the B_1-O bond is stronger than the B_2-O bond.

The calculated atomic Mulliken charges[74] obtained with the different approaches are given in Table 5. In general, the absolute values of the calculated charges are slightly larger than the effective charges derived from the LO−TO splitting in Raman spectra.[61] Calculated and experimental Li charges q_{Li} range between +0.8 and +1.0. Only the semiempirical method MSINDO gives a smaller charge, +0.42. The effective charge of boron, q_B^{eff}, is +1.2, while the calculated charges, q_B, range from 1.1 to 1.7. Accordingly, the calculated oxygen charges are with −0.8 to −1.2 mostly more negative than $q_O^{eff} \approx -0.9$. The PWGGA method in CRYSTAL gives a less ionic description of LTB than HF+PW. As expected, the results of the hybrid methods PW1PW and B3LYP are intermediate. The core

TABLE 5: Comparison of Calculated Mulliken Charges q of Atoms in the Primitive LTB Cell with Effective Charges q^{eff} Derived from Raman Spectroscopy[61]

atom	HF + PW[a]	PWGGA[a]	PWGGA-PAW[b]	PWGGA-US[c]	PW1PW[a]	B3LYP[a]	MSINDO[d]	expt
Li	0.89	0.84	0.97	0.97	0.85	0.85	0.41	0.8 ± 0.1
B_1	1.72	1.28	1.48	1.54	1.38	1.41	1.08	
B_2	1.71	1.32	1.64	1.67	1.40	1.45	1.18	
B_{av}	1.71	1.30	1.56	1.61	1.39	1.43	1.13	1.23 ± 0.05
O_1	−1.19	−0.94	−1.24	−1.19	−1.01	−1.03	−0.72	
O_2	−1.22	−0.97	−1.27	−1.21	−1.02	−1.04	−0.76	
O_3	−1.31	−1.05	−1.28	−1.22	−1.11	−1.12	−0.77	
O_4	−1.18	−0.96	−1.24	−1.19	−1.00	−1.03	−0.82	
O_{av}	−1.23	−0.98	−1.26	−1.21	−1.03	−1.06	−0.77	-0.93 ± 0.01

[a] CRYSTAL results with basis set A. [b] VASP results with cutoff energy 600 eV. [c] VASP results with cutoff energy 594 eV. [d] Cyclic cluster $Li_{16}B_{32}O_{56}$; Löwdin analysis of orthogonal basis.

potential has little influence on the charge distribution, as can be seen by the similarities between PWGGA-PAW and PWGGA-US (Table 5). The PWGGA results obtained with CRYSTAL and VASP are slightly different which is due to basis set dependence of Mulliken charge analysis.

4. Summary and Conclusions

The structural, energetic and electronic properties of lithium tetraborate were investigated by means of periodic quantum-chemical calculations. The results of six DFT-type methods and the semiempirical method MSINDO were compared among each other and to available literature data. The comparison of optimized structural parameters with experiment shows that the hybrid methods PW1PW and B3LYP give best results for lattice parameters, bond lengths and angles. Other methods (HF+PW, PWGGA, PWGGA-PAW, PWGGA-US, and semiempirical MSINDO) give similar deviations from experimental data. However, it should be noted that all deviations are small (less than 1.8% for lattice parameters and 2.6% for bond lengths and angles).

The comparison of PWGGA results in a LCAO and two plane wave implementations revealed that the basis set dependence of geometry parameters and the band structure is small, but is more pronounced for energetic properties. The calculated cohesive energies of LTB have a large scattering. They range from −7200 to −8100 kJ/mol. Very close agreement with the experimental heat of atomization is obtained with PW1PW.

The calculations of electronic properties show that $Li_2B_4O_7$ is an insulator with a wide indirect band gap. From earlier investigations of a related lithium borate, LiB_3O_5, and from the FA edge of LTB, we estimated the LTB band gap as 9.0 eV. The calculated band gaps of the hybrid methods PW1PW (E_g = 8.88 eV) and B3LYP (E_g = 8.85 eV) by using basis set B have best agreement with this estimated value. The results of other methods show that MSINDO gives better band gap (9.7 eV) than HF+PW (17.68 eV), PWGGA (6.76 eV), PWGGA-US (6.3 eV), and PWGGA-PAW (6.2 eV). The choice of atomic basis sets in the LCAO approach has a notable effect on the calculated electronic structure. The LTB band gap is reduced by 0.3−0.5 eV when diffuse orbitals are added to the basis set of Li and B.

From an analysis of the electronic charge density distribution, it is concluded that B_1−O and B_2−O are mainly covalent bonds, and the Li−O bond is ionic. This agrees with similar analysis of LiB_3O_5. Calculated effective Mulliken charges for all atoms are in good agreement with charges derived from the LO−TO splitting in Raman spectra.

For future studies of defect properties of lithium tetraborate a differentiated picture emerges. Only one method, HF+PW, can be discarded because it gives the largest deviations from experimental data and from the other methods for all investigated properties. Some care has to be taken with the semiempirical method MSINDO, but the overall agreement with the DFT results is good so that at least qualitative trends should be reproduced correctly. The overall best quantum description is given by the hybrid methods PW1PW and B3LYP, where PW1PW is slightly better for geometrical parameters and considerably closer to experimental cohesive energies. The PWGGA DFT method shows larger deviations for energetic and electronic properties. On the other hand, pure DFT calculations are computationally less costly than hybrid calculations. Their efficiency is further increased by using plane waves as basis functions. Therefore, the choice of the method, PW1PW, PWGGA, or MSINDO, will depend on the complexity of the system and the focus of the study.

Acknowledgment. This work was supported by the Deutscher Akademischer Austauschdienst (V.V.M.) and the State of Lower Saxony, Germany, by a "Georg Christoph Lichtenberg" fellowship (M.M.I.). The authors are grateful to Prof. H. Pfnür for support in performing this work. M.M.I. is thankful to Prof. A. Savin for valuable discussion and V.V.M. is thankful to Dr. V. M. Holovey for valuable comments.

References and Notes

(1) Komatsu, R.; Sugawara, T.; Watanabe, N. *Rev. Laser Eng.* **1999**, *27*, 541.

(2) Whatmore, R. W.; Shorrocks, N. M.; O'Hara, C.; Ainger, F. W.; Young, I. M. *Electron. Lett.* **1981**, *17*, 11.

(3) Komatsu, R.; Sugawara, T.; Sassa, K.; Sarukura, N.; Liu, Z.; Izumida, S.; Segawa, Y.; Uda, S.; Fukuda, T.; Yamanouchi, K. *Appl. Phys. Lett.* **1997**, *70*, 3492.

(4) Sugawara, T.; Komatsu, R.; Uda, S. *Solid State Commun.* **1998**, *107*, 233.

(5) Adachi, M.; Nakazawa, K.; Kawabata, A. *Ferroelectrics* **1997**, *195*, 123.

(6) Filipiak, J.; Majchrowski, A.; Lukasiewicz, T. *Arch. Acoust.* **1994**, *19*, 131.

(7) Bhalla, A. S.; Cross, L. E.; Whatmore, R. W. *Jpn. J. Appl. Phys.* **1985**, *24*, 727.

(8) Kim, C.-S.; Park, J.-H.; Moon, B. K.; Seo, H.-J.; Choi, B.-Ch.; Hwang, Y.-H.; Kim, H. K.; Kim, J. N. *J. Appl. Phys.* **2003**, *94*, 7246.

(9) Kim, C.-S.; Kim, D. J.; Hwang, Y.-H.; Kim, H. K.; Kim, J. N. *J. Appl. Phys.* **2002**, *92*, 4644.

(10) Rizak, I. M.; Rizak, V. M.; Baisa, N. D.; Bilanich, V. S.; Boguslavskii, M. V.; Stefanovich, S. Yu.; Golovei, V. M. *Crystallogr. Rep.* **2003**, *48*, 676.

(11) Rizak, V. M.; Rizak, I. M.; Bausa, N. D.; Bilanych, V. S.; Stefanovich, S. Yu. Bohuslavskii, M. B.; Holovey, V. M. *Ferroelectrics* **2003**, *286*, 49.

(12) Kim, C.-S.; Hwang, Y. H.; Kim, H. K.; Kim, J. N. *Phys. Chem. Glass.* **2003**, *44*, 166.

(13) Button, D. P.; Mason, L. S.; Tuller, H. L.; Uhlmann, D. R. *Solid State Ionics* **1983**, *9/10*, 585.

(14) Paul, G. L.; Taylor, W. *J. Phys. C* **1982**, *15*, 1753.

(15) Vij, D. R., Ed.; *Thermoluminescent Materials*, PTR Prentice-Hall: Englewood Cliffs, NJ, 1993 452.

(16) Radaev, S. V.; Muradyan, L. A.; Malakhova, L. F.; Burak, Ya. V.; Simonov, V. I. *Kristallografiya* **1989**, *34*, 1400.
(17) Ogorodnikov, I. N.; Pustovarov, V. A.; Kurzhalov, A. V.; Isaenko, L. I.; Kirm, M.; Zimmerer, G. *Phys. Solid State* **2000**, *42*, 464.
(18) Kuznetsov, A. Y.; Kruzhalov, A. V.; Ogorodnikov, I. N.; Sobolev, A. B.; Isaenko, L. I. *Phys. Solid State* **1999**, *41*, 48.
(19) Burak, Ya. V.; Dovgii, Ya. O.; Kityk, I. V. *Sov. Phys. Solid State* **1989**, *31*, 1634.
(20) Indris, S.; Heitjans, P.; Roman, H.; Bunde, A. *Phys. Rev. Lett.* **2000**, *84*, 2889.
(21) Indris, S.; Heitjans, P. *J. Non-Cryst. Solids* **2002**, *307*−*310*, 555.
(22) Perdew, J. P.; Wang, Y. *Phys. Rev. B* **1992**, *45*, 13244.
(23) Bredow, T.; Gerson, A. R. *Phys. Rev. B* **2000**, *61*, 5194.
(24) Perdew, J. P.; Chevary, J. A.; Vosko, S. H.; Jackson, K. A.; Penderson, M. R.; Singh, D. J.; Fiolhais, C. *Phys. Rev. B* **1992**, *46*, 6671.
(25) Gerson, A. R.; Bredow, T.; Pacchioni, G.; Simpson, D. J.; Jones, R. *Int. J. Ionics* **2001**, *7*, 290.
(26) Becke, A. D. *J. Chem. Phys.* **1993**, *98*, 5648.
(27) Saunders, V. R.; Dovesi, R.; Roetti, C.; Orlando, R.; Zicovich-Wilson, C. M.; Harrison, N. M.; Doll, K.; Civalleri, B.; Bush, I.; D'Arco, Ph.; Llunell, M. *CRYSTAL2003 User's Manual*; University of Torino, Torino, Italy, 2003.
(28) Ojamäe, L.; Hermansson, K.; Pisani, C.; Causà, M.; Roetti, C. *Acta Crystallogr. B* **1994**, *50*, 268.
(29) Prencipe, M.; Zupan, A.; Dovesi, R.; Aprà, E.; Saunders, V. R. *Phys. Rev. B* **1995**, *51*, 3391.
(30) Orlando, R.; Dovesi, R.; Roetti, C. *J. Phys.: Condens. Matter* **1990**, *2*, 7769.
(31) Binkley, J. S.; Pople, J. A.; Hehre, W. J. *J. Am. Chem. Soc.* **1980**, *102*, 939.
(32) Catti, M.; Valerio, G.; Dovesi, R.; Causà, M. *Phys. Rev. B* **1994**, *49*, 14179.
(33) Bredow, T.; Heitjans, P.; Wilkening, M. *Phys. Rev. B* **2004**, *70*, 115111.
(34) Kresse, G.; Hafner, J. *Phys. Rev. B* **1993**, *47*, 558.
(35) Kresse, G.; Hafner, J. *Phys. Rev. B* **1993**, *48*, 13115.
(36) Kresse, G.; Hafner, J. *Phys. Rev. B* **1994**, *49*, 14251.
(37) Vanderbilt, D. *Phys. Rev. B* **1990**, *41*, 7892.
(38) Kresse, G.; Hafner, J. *J. Phys.: Condens. Matter* **1994**, *6*, 8245.
(39) Kresse, G.; Joubert, J. *Phys. Rev. B* **1999**, *59*, 1758.
(40) Blöchl, P. E. *Phys. Rev. B* **1994**, *50*, 17953.
(41) VASP guide: http://cms.mpi.univie.ac.at/vasp/vasp/vasp.html.
(42) Ahlswede, B.; Jug, K. *J. Comput. Chem.* **1998**, *20*, 563.
(43) Ahlswede, B.; Jug, K. *J. Comput. Chem.* **1998**, *20*, 572.
(44) Nanda, D. N.; Jug, K. *Theor. Chim. Acta* **1980**, *57*, 93.
(45) Bacon, A. D.; Zerner, M. C. *Theor. Chim. Acta* **1979**, *53*, 21.
(46) Jug, K.; Bredow, T. *Encyclopedia of Computational Chemistry*; Schleyer, P. v. R., Allinger, N. L., Clark, T., Gasteiger, J., Kollman, P. A., Schaefer, H. F., III., Schreiner, P. R., Eds.; Wiley: New York, 1998; Vol. 4; p 2599.
(47) Bredow, T.; Jug, K. *Surf. Sci.* **1995**, *327*, 398.
(48) Jug, K.; Geudtner, G. *J. Chem. Phys.* **1996**, *105*, 5285.
(49) Jug, K.; Geudtner, G. *J. Mol. Catal. A* **1997**, *119*, 143.
(50) Bredow, T. *Surf. Sci.* **1998**, *401*, 82.
(51) Ahlswede, B.; Jug, K. *J. Comput. Chem.* **1999**, *20*, 563.
(52) Gerson, A. R.; Bredow, T. *Phys. Chem. Chem. Phys.* **1999**, *1*, 4889.
(53) Tikhomirov, V. A.; Jug, K. *J. Phys. Chem. B* **2000**, *104*, 7619.
(54) Ahlswede, B.; Homann, T.; Jug, K. *Surf. Sci.* **2000**, *445*, 49.
(55) Steveson, M.; Bredow, T.; Gerson, A. R. *Phys. Chem. Chem. Phys.* **2002**, *4*, 358.
(56) Homann, T.; Bredow, T.; Jug, K. *Surf. Sci.* **2002**, *515*, 205.
(57) Geudtner, G.; Jug, K. *Z. Anorg. Allg. Chem.* **2003**, *629*, 1731.
(58) Janetzko, F.; Bredow, T.; Jug, K. *J. Chem. Phys.* **2002**, *116*, 8994.
(59) Bredow, T.; Geudtner, G.; Jug, K. *J. Comput. Chem.* **2001**, *22*, 861.
(60) Jug, K.; Bredow, T. *J. Comput. Chem.* **2004**, *25*, 1551.
(61) Vdovin, A. V.; Moiseenko, V. N.; Gorelik, V. S.; Burak, Ya. V. *Phys. Sol. State* **2001**, *43*, 1648.
(62) Kubaschewski, O.; Alock, C. B.; Spencer, P. J. *Materials Thermochemistry*, 6th ed.; Pergamon Press: New York, 1992; p 288.
(63) Vosko, S. H.; Wilk, L.; Nusair, M. *Can. J. Phys.* **1980**, *58*, 1200.
(64) Kovalev, O. V. *Representations of the Crystallographic Space Groups: Irreducible Representations, Induced Representations, and Corepresentations*; Gordon and Breach: Philadelphia, PA, 1993.
(65) Li, D.; Ching, W. Y. *Phys. Rev. B* **1996**, *54*, 13616.
(66) Hsu, W. Y.; Kasowski, R. V. *J. Appl. Phys.* **1993**, *73*, 4101.
(67) Li, J.; Duan, C.-G.; Gu, Z.-Q.; Wang, D.-S. *Phys. Rev. B* **1998**, *57*, 6925.
(68) Cheng, W.-D.; Chen, J.-T.; Lin, Q.-S.; Zhang, Q.-E.; Lu, J.-X. *Phys. Rev. B* **1999**, *60*, 11747.
(69) Xu, Y.-N.; Ching, W.; French, R. *Phys. Rev. B* **1993**, *48*, 17695.
(70) French, R. H.; Ling, J. W.; Ohuchi, F. S.; Chen, C. T. *Phys. Rev. B* **1991**, *44*, 8496.
(71) Pisani, C.; Dovesi, R.; Roetti, C. *Hartree*−*Fock ab initio Treatment of Crystalline Systems*; Lecture Notes in Chemistry 48, Springer-Verlag: Heidelberg, Germany, 1988.
(72) Monkhorst, H. J.; Pack, J. D. *Phys. Rev.* **1976**, *13*, 5188.
(73) Bader, R. F. W. *Atoms in molecules: a quantum theory*; Oxford University Press: New York, 1990.
(74) Mulliken, R. S. *J. Chem. Phys.* **1955**, *23*, 1833.